JOURNAL OF MATERIALS SCIENCE **38** (2003) 1493–1498

Grain size effects in the charpy impact energy of a thermally embrittled RPV steel

J. R. TARPANI*, D. SPINELLI
Materials, Aeronautical and Automotive Engineering Department–SMM, Engineering School of São Carlos–EESC, University of São Paulo–USP, Av. Trabalhador São Carlense 400, São Carlos-SP, 13566-590, Brazil
E-mail: jrpan@sc.usp.br

The Charpy impact energies of a reactor pressure vessel (RPV) steel in the as-received and several thermally embrittled conditions have been assessed on the basis of microstructural parameters. It has been concluded that the parameters controlling the impact-absorbed energy of pre-cracked and side-grooved Charpy test specimens are the equivalent grain size of dual-phase annealed microstructures, and the bainite packet size of single-phase quenched and tempered materials. The Charpy energy has been correlated very well with the reduction in area and true fracture strain of tensile specimens, which could be inferred as grain size governed mechanical properties.

Nomenclature

a_0	Initial crack length (mm)
A-H, J, L, N	Microstructure nomination
AC	Air cooling
ASTM	American Society for Testing and Materials
B_G	Gross thickness (mm)
BHN	Brinell hardness number
CIE	Charpy impact energy of pre-cracked side-grooved bend bars (Joules)
$D_{bainite}$	Mean diameter of bainite grain or packet (μm)
$D_{ferrite}$	Mean diameter of ferrite grain (μm)
D_0	Original diameter (mm)
EGS	Equivalent grain size (μm)
EL	Elongation at fracture (%)
FC	Furnace cooling
K	Linear elastic stress intensity factor (MPa$\sqrt{\text{m}}$)
L_0	Original gage length (mm)
n	Strain-hardening exponent
Q&T	Quenching and tempering
r	Correlation coefficient
RA	Reduction in area at fracture (%)
RCS	Representative cell size (μm)
RPV	Reactor pressure vessel
SG	Side-groove level (%)
S_U	Nominal ultimate tensile strength (MPa)
S_Y	Nominal yield strength (MPa)
T	Plate thickness (inches)
T-L	Transversal-longitudinal orientation
W	Specimen width (mm)
WQ	Water quenching
ε_f	True fracture strain (%)
ε_f	True fracture stress (MPa)

1. Scope

In this work, a nuclear grade steel was submitted to several heat treatment routes, viz. annealing and quenching and tempering, aimed at obtaining a range of elastic-plastic fracture resistance under dynamic loading conditions. Thermal cycles were designed to simulate the mechanical behavior of structural steels undergoing neutron dose damage in radioactive environments, e.g., reactor pressure vessel (RPV) steels [1, 2]. The principal objective of this study was to confirm a Hall-Petch dependence of Charpy energy on grain size in the moderate strain-rate regimen, as generated by impact velocities of order of 5 m/s. For this purpose, pre-cracked and side-grooved Charpy bend bars were tested in an instrumented impact testing machine, and the net absorbed energy during the overall fracture process was tentatively correlated to the significant microstructural parameters of the heat treated materials.

2. Material

The Brazilian ASTM A508 Class 3A steel is an exceptionally high-toughness microalloyed RPV material (chemistry in Table I) designed for the nuclear industry. The as-received material exhibits a Charpy impact energy far exceeding 300 Joules when conventional notched bend bar specimens are tested as ambient temperature. Shown in Fig. 1 is the original microstructure (A), which is basically comprised of globular bainite 8.5 ASTM grain size number. Fig. 1 also pictures some of

*Author to whom all correspondence should be addressed.

TABLE I Chemical composition determined for the A508 nuclear grade steel (wt%)

C	Si	Mn	Ni	Mo	Cr	Al	P	S
0.19	0.24	1.30	0.72	0.51	0.03	0.012	0.007	0.009

the embrittled microstructures obtained through special heat treatments applied to the as-received A508 steel, which are described in Table II. Two classes of thermally embrittled materials are exemplified: dual-phase ferrite/bainite microstructures, designated *B* and *E*, which were obtained from annealing heat treatments, and single-phase tempered bainite, J and L, produced by quenching and tempering (Q&T).

Table III lists the microstructural parameters of the materials tested. As expected, ferrite and bainite grain sizes enlarged with the severity of the annealing heat treatment, and a quite outstanding acceleration of bainite grain size is noticed for the microstructures *G* and *H*. It can be seen that milder annealing cycles generate both phases in a fixed proportion, of about 1:1, but in the latter microstructures there exist far more bainite than ferrite. Higher austenitization temperatures, providing larger prior austenite grain size in these microstructures, gave rise to higher hardenabilities, and corresponding microstructural refinement, thus preventing the nucleation of the pro-eutectoid ferrite phase during furnace cooling. Accordingly, a trade-off between grain size and microstructural refinement, the latter denoted by the acicularization of the bainite phase, is likely to occur due to increasing austenitization temperature.

TABLE II Annealing and Q&T thermal cycles applied to the original A508 steel

	Thermal cycle
Annealing route	
B	900°C/1 h + furnace cooling (FC)
C	950°C/1.5 h + FC
D	1000°C/2 h + FC
E	1050°C/2.5 h + FC
F	1100°C/3 h + FC
G	1150°C/3.5 h + FC
H	1200°C/1 h + FC
Quenching and tempering route	
A (as-received)	920°C/7 h + air cooling (AC); 905°C/7 h + water quenching (WQ); 655°C/12 h + AC; 550°C/30 h + FC; 600°C/10 h + FC; 600°C/10 h + FC
J	920°C/3 h + AC; 920°C/1 h + WQ; 990°C/1 h + WQ; 575°C/2 h + FC
L	1300°C/1 h + FC;1100°C/2 h + WQ; 615°C/1 h + FC
N	920°C/2 h + AC; 905°C/2 h + WQ; 655°C/1.5 h + FC

TABLE III Microstructural parameters and phase percentages of test materials. ASTM grain size number is given in parentheses

Annealing route	$D_{ferrite}$ (μm)	$D_{bainite}$ (μm)	Phase % ferrite/bainite
B	20 (8.3)	19 (8.5)	48/52
C	30 (7.2)	26 (7.6)	49/51
D	39 (6.4)	50 (5.7)	50/50
E	47 (5.9)	56 (5.4)	50/50
F	50 (5.7)	64 (5.0)	51/49
G	55 (5.4)	475 (0)	19/81
H	61 (5.1)	817 (00)	11/89

Quenching and tempering route	$D_{bainite}$(μm)
A(as-received)	19 (8.6)
J	105 (3.5)
L	153 (2.5)
N	25 (7.7)

TABLE IV Conventional mechanical properties ((BHN at room temperature, tensile properties at 300°C) determined for the as-received (*A*) and thermally embrittled materials (B-N)

	BHN (100 kgf)	S_Y (MPa)	S_U (MPa)	EL[a] (%)	RA (%)	*n*
Annealing route						
B	170	360	620	17	71	0.20
C	167	345	610	16	63	0.20
D	168	370	620	12	54	0.20
E	169	375	625	12	49	0.20
F	192	450	675	11	39	0.14
G	198	470	685	05	31	0.15
H	208	490	665	05	28	0.16
Q&T route						
A(as-received)	175	400	555	11	77	0.16
J	269	725	865	07	61	0.09
L	246	700	810	08	44	0.09
N	212	535	700	11	73	0.15

[a] $L_0 \simeq 40$ mm $\simeq 10\ D_0$.

Table III shows that a considerable range of grain sizes was also obtained by quenching and tempering the original A508 steel.

Hardness measurements at ambient temperature and tensile tests at 300°C were carried out for the materials, and results are supplied in Table IV. From the data it can be noticed that Q&T microstructures are substantially stronger than annealed ones.

3. Experimental

Charpy bend bar testpieces ($10 \times 10 \times 55$ mm^3) were machined from the one-quarter-thickness position ($T/4$) of the as-received and heat treated forged plates in T-L orientation. They were fatigue pre-cracked to a nominal 0.5 a_0/W ratio, where a_0 is the initial crack length and $W = 10$ mm is the specimen width, and side-grooved (SG) to 20% and 33% of the specimen gross-thickness, $B_G = 10$ mm. Special care was taken during the pre-cracking procedure to comply exactly with the requirements established in [3, 4] regarding to the maximum stress intensity factor-K developed at crack tip. Charpy testpieces were impacted at 300°C in an instrumented testing machine using a 300 Joules hammer travelling at a velocity of 5.52 m/s. The absorbed energy was digitally recorded, which accounted for energy losses due to friction, windage and specimen tossing, i.e., the net absorbed energy

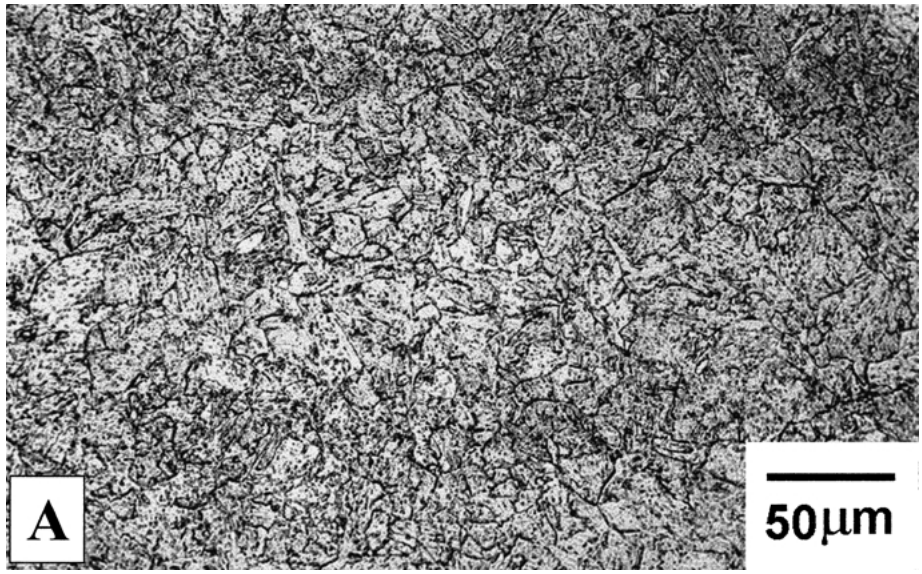

(a)

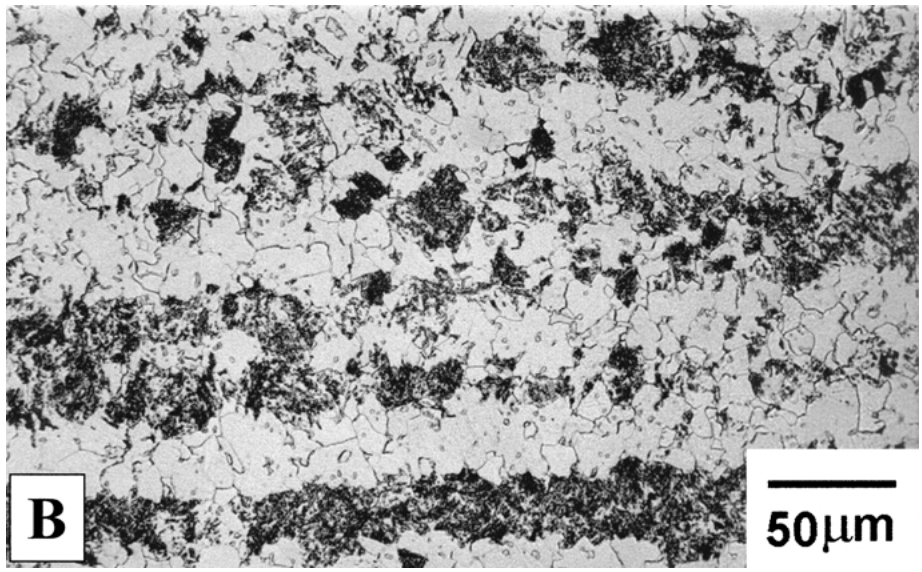

(b)

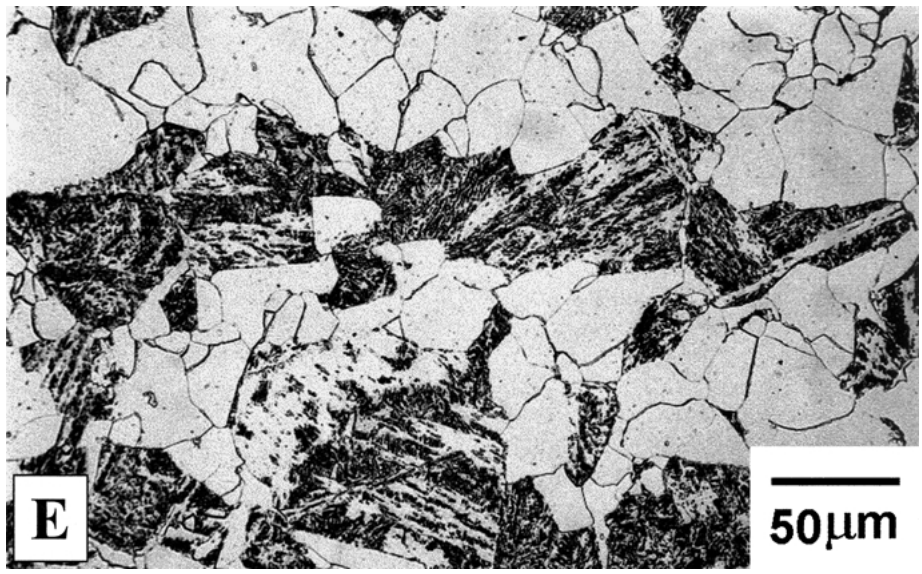

(c)

Figure 1 Light micrographs of some materials tested: (a) As-received condition *A*, (b) *B* and (c) *E* are annealed materials, (d) *J* and (e) *L* are Q&T microstructures. Etched in Nital. (*Continued*)

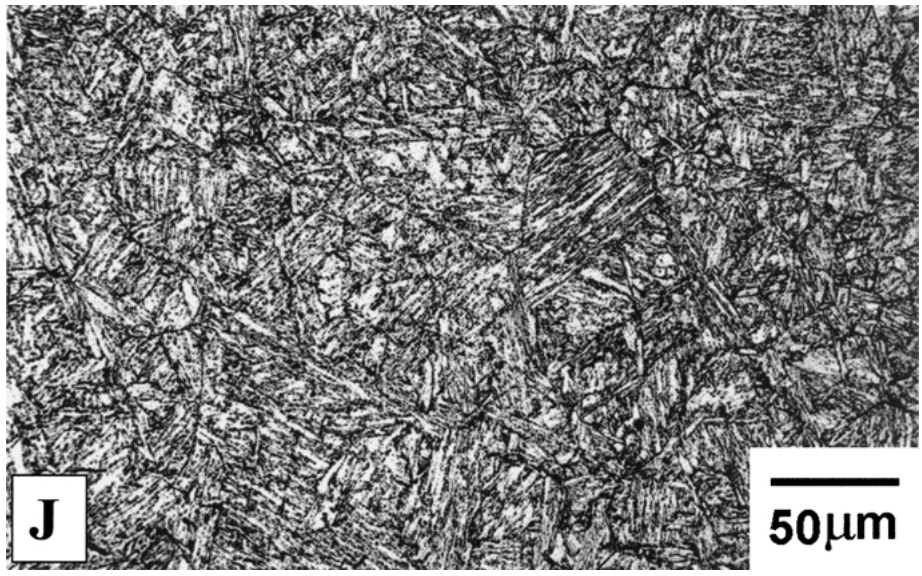

(d)

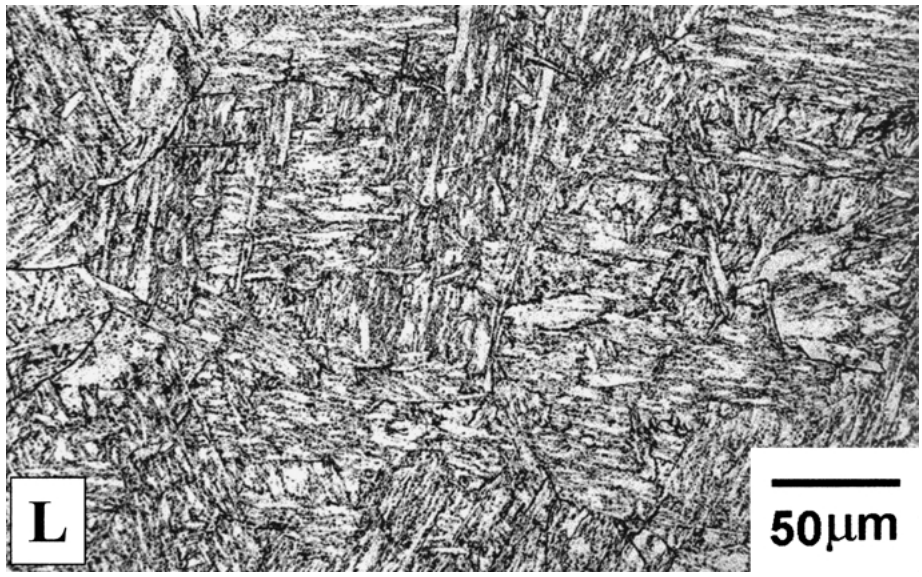

(e)

Figure 1 (*Continued*).

was obtained. As a general rule, three testpieces were tested for each testing condition, so that the Charpy energy results provided herein always refer to the mean values.

4. Results and discussion

Fig. 2a plots the relationship between the reduction in area of tensile specimens, RA, and the inverse of the square root of the representative cell size, RCS, of dual-phase ferrite/bainite (annealed) and single phase tempered bainite (Q&T) microstructures. It should be observed that for dual-phase annealed materials, the RCS value has been taken as the equivalent grain size (EGS) of the microstructures, which has been proposed as a volume-fraction weighted average of the grain sizes (diameters) of both individual phases, ferrite and bainite, thus resembling composite materials, as follows [5]:

$$\text{EGS} = ((D_{\text{ferrite}}) \cdot (\%\,\text{Ferrite}) + (D_{\text{bainite}}) \cdot (\%\,\text{Bainite}))/100 \quad (1)$$

where the ferrite and bainite grain sizes, respectively D_{ferrite} and D_{bainite}, are supplied in Table III along with the corresponding phase percentages. Good correlation is observed in Fig. 2a for both sets of data points, as denoted by the coefficient r, and so a Hall-Petch dependence [6, 7] of RA on RCS can be ascertained.

Shown in Fig. 2b is the relationship between the true fracture strain, ε_{f}, of tensile specimens and the RCS value, where ε_{f} is obtained from RA as follows:

$$\varepsilon_{\text{f}}[1 - (\text{RA}/100)]^{-1} \quad (2)$$

A Hall-Petch dependence of ε_{f} on RCS is clearly noticed in Fig. 2b, corroborating previous findings by Armstrong [8].

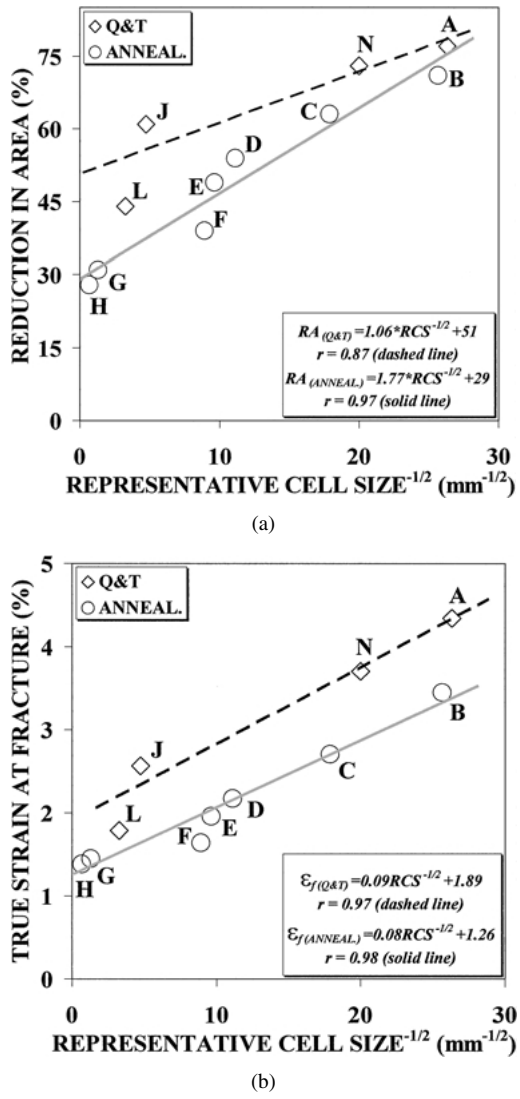

Figure 2 A Hall-Petch dependence for the reduction in area (a) and true fracture strain and (b) dependence on grain size for the materials tested.

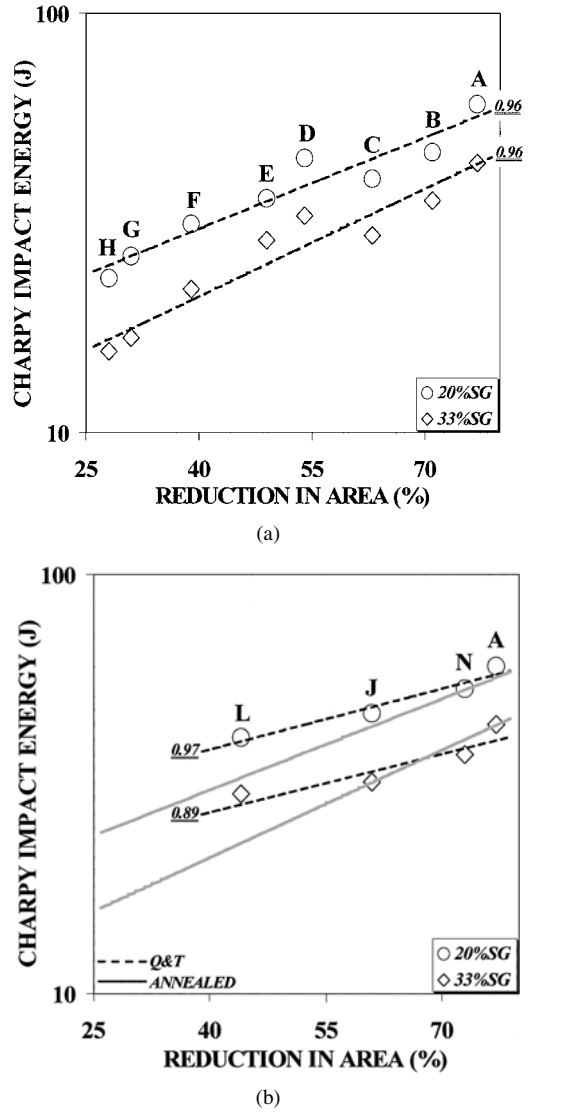

Figure 3 Relationship between Charpy impact energy and reduction in area for annealed (a) and Q&T (b) microstructures. In (b), a baseline is drawn from results of annealed materials.

Fig. 3 displays the relationship between RA and the Charpy impact energy, CIE, determined for annealed and Q&T microstructures. The correlation of both sets of data points is encouraging, indicating that CIE may be grain size governed as well. Fig. 3 indirectly establishes the dependence of CIE on the representative cell size concept, RCS, as long as RA, and consequently ε_f have already been proven to strongly depend on that parameter (Fig. 2). In fact, since CIE values are upper shelf energies they should scale with the product $\varepsilon_f \cdot \sigma_f$, where σ_f is the true fracture stress, and therefore a Hall-Petch dependence of CIE on RCS would not be surprising.

In Fig. 4, this expected dependence of CIE on RCS is shown according to a Hall-Petch relationship. Data correlation is very auspicious, mainly if one considers the simplest rule of mixture adopted for estimation of RCS (or identically EGS) of annealed materials (Equation 1).

Recalling the EGS concept, Equation 1, an unexpected behavior is noticed in Fig. 4a, for the microstructure *D*, in which the fracture energy increases with increasing grain size. In can be observed that this microstructure, despite being coarser than *C* (Table III), presents a significantly better dynamic performance than the latter. This behavior can be explained in terms of the major role played by the bainite phase refinement over the equivalent grain size concept, as long as they are competitive mechanisms affecting the mechanical behavior of annealed microstructures, as previously noted.

Figs 3b and 4b indicate that, given fixed RA and RCS values, respectively, the annealed microstructures exhibit a poorer dynamic fracture performance as compared to Q&T ones.

It should be emphasized that the correlation between quasi-static J-elastic plastic fracture mechanics properties and grain size has been proposed in the literature [9, 10], invariably on the basis of the widely accepted Hall-Petch type relationship and for single-phase metallic materials only. The present study has successfully applied such an approach over a wide range of grain sizes of single- and dual-phase microstructures of a structural nuclear grade steel, when the net absorbed energy under impact loading regimen is the chief concern. Hence, one could infer the existence of

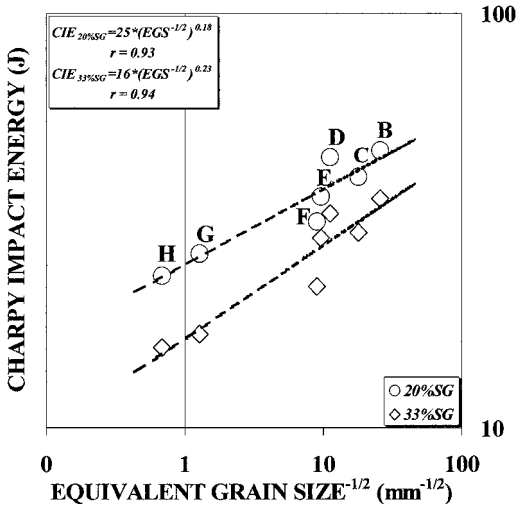

(a)

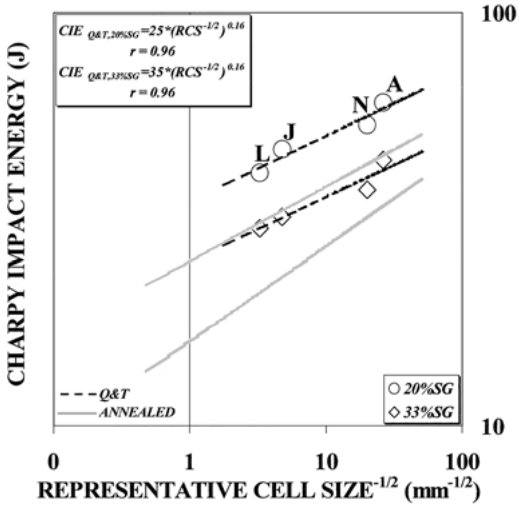

(b)

Figure 4 A Hall-Petch dependence for the Charpy impact dependence on grain size for annealed (a) and Q&T (b) microstructures. In (b), a baseline is drawn from results of annealed materials.

a straightforward correlation between the Charpy impact energy and the quasi-static J-integral parameter for these materials, as vastly suggested in the literature [11–16].

5. Concluding remarks

The Charpy impact energies of the as-received and several thermally embrittled conditions of a reactor pressure vessel (RPV) steel have been assessed on the basis of microstructural parameters. It has been concluded that the parameters controlling the energy absorption capacity during the dynamic fracture process of bend bar specimens are the equivalent grain size of dual-phase ferrite/bainite annealed microstructures and the tempered bainite packet size of single-phase Q&T microstructures. This dependence of the Charpy impact energy on the representative cell size of the microstructures tested has been disclosed as a Hall-Petch relationship. The same findings have been extended to conventional mechanical properties obtained in traditional tensile testing, like reduction in area and true fracture strain.

Acknowledgments

The authors thankfully acknowledge the financial support provided by FAPESP—Fundação para o Amparo à Pesquisa do Estado de São Paulo (Contracts 97/05652-1 and 99/09431-5).

References

1. K. ONIZAWA, K. FUKAIA, Y. NISHIYAMA, M. SUZUKI, S. KAIHARA and T. NAKAMURA, *Int. J. Press Vessels Piping* **70** (1997) 201.
2. E. VITALE and M. BEGHINI, *ibid.* **46** (1991) 289.
3. ANON., "Annual Book of ASTM Standards," Designation E23 (1997).
4. *Idem.*, "Annual Book of ASTM Standards," Designation E1820 (1997).
5. J. R. TARPANI, W. W. BOSE FILHO and D. SPINELLI, *J. Mater. Eng. Perf.* **11** (2002) 414.
6. N. J. PETCH, *J. Iron Steel Inst.* **174** (1953) 25.
7. E. O. HALL, *Proc. Phys. Soc.* B **64** (1951) 747.
8. R. W. ARMSTRONG, *Trans. Indian Inst. Met.* **50** (1997) 521.
9. M. SRINIVAS, G. MALAKONDAIAH, R. W. ARMSTRONG and P. R. RAO, *Acta Metall. Mater.* **39** (1991) 807.
10. *Idem.*, *Eng. Fract. Mech.* **28** (1987) 561.
11. K. WALLIN, *Fatig. Fract. Eng. Mater. Struct.* **24** (2001) 537.
12. P. C. GIOIELLI, J. D. LANDES, P. C. PARIS, H. TADA and L. LOUSHIN, ASTM STP (Special Technical Publication) Vol. **1360** (2000) p. 61.
13. P. C. PARIS and R. E. JOHNSON, ASTM STP 803, Vol. **2** (1983) p. 5.
14. K. KUSSMAUL and L. ISSLER, ASTM STP 803, Vol. **2** (1983) p. 41.
15. F. J. LOSS, B. H. MENKE, A. L. HISER and H. E. WATSON, ASTM STP 803 Vol. **2** (1983) 777.
16. D. M. NORRIS, J. E. REAUGH and W. L. SERVER, ASTM STP, Vol. **743** (1981) p. 207.

Received 21 March
and accepted 11 December 2002